

We are IntechOpen, the world's leading publisher of Open Access books Built by scientists, for scientists

4,400

Open access books available

118,000

International authors and editors

130M

Downloads

Our authors are among the

154

Countries delivered to

TOP 1%

most cited scientists

12.2%

Contributors from top 500 universities



WEB OF SCIENCE™

Selection of our books indexed in the Book Citation Index
in Web of Science™ Core Collection (BKCI)

Interested in publishing with us?
Contact book.department@intechopen.com

Numbers displayed above are based on latest data collected.
For more information visit www.intechopen.com



Resonant Power Converters

Mohammed Salem and Khalid Yahya

Abstract

Recently, DC/DC resonant converters have received much research interest as a result of the advancements in their applications. This increase in their industrial application has given rise to more efforts in enhancing the soft-switching, smooth waveforms, high-power density, and high efficiency features of the resonant converters. Their suitability to high frequency usage and capacity to minimize switching losses have endeared them to industrial applications compared to the hard-switching conventional converters. However, studies have continued to suggest improvements in certain areas of these converters, including high-power density, wide load variations, reliability, high efficiency, minimal number of components, and low cost. In this chapter, the resonant power converters (RPCs), their principles, and their classifications based on the DC-DC family of converters are presented. The recent advancements in the constructions, operational principles, advantages, and disadvantages were also reviewed. From the review of different topologies of the resonant DC-DC converters, it has been suggested that more studies are necessary to produce power circuits, which can address the drawbacks of the existing one.

Keywords: soft-switching, LLC resonant converter, control strategies, resonant power converters (RPCs),

1. Introduction

Several studies have been conducted on the switching mode DC-DC converters to ensure that they satisfy the most demanding criteria for power electronics application. The possibility of minimizing the switching and conduction losses in the switch-mode through increasing the switching frequency makes them more attractive. However, several switching topologies can attain a high-power transfer [1, 2] but the problem is the power switches (transistors or MOSFET), diodes, and energy storage passive elements (capacitors and inductors) contained in the structure of the power converters, which affects their efficiency. Efficient circuits have been developed for power converters along with the developments in materials, control systems, and devices technology. Such topologies can minimize the overall converter size and the switching losses, thereby, providing a higher efficiency [3–5]. The DC-DC converters can be categorized into three major groups (linear, hard-switching, and soft-switching mode resonant converters) based on their modes of operation as depicted in **Figure 1** [6–8].

The advantages of the linear regulator technologies include low noise, fast response, simplicity, and excellent regulation. However, they have some disadvantages such as power dissipation in any working condition, which can result in low efficiency. The switching-mode topologies can be categorized based on the isolation

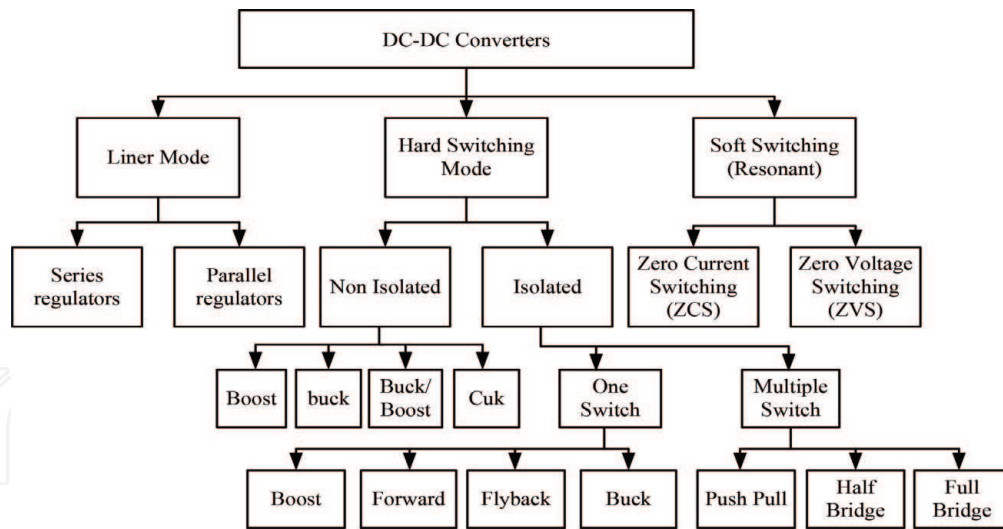


Figure 1.
The classification of the DC-DC converters.

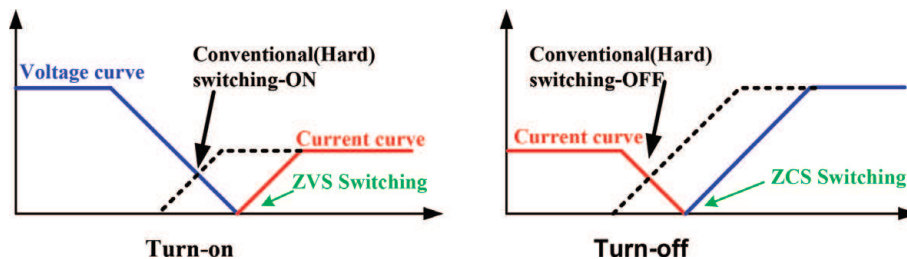


Figure 2.
Current waveform and voltage waveform of hard-switching and soft-switching at both turn-on and turn-off transitions.

feature to galvanic isolation converter, which also called chopper, and non-isolated converter. Galvanic isolation is required in most applications during the process of converting the power from the utility grid (voltages ranging from 100 to 600 V) for safety reason [9–11]. Since a higher power transformer is required in these converters, the single-switch converter may not be a proper solution for higher power applications, and as such, the other DC-DC isolated converters with more than one switch, such as the push-pull and full or half-bridge converters, are more appropriate for such high-power applications. Hard-switching transitions in devices operating with switched-mode converters will result in high power dissipation and a gradual reduction of the efficiency of the converter; it can damage the switching devices as well. Snubbers are used to reduce the stress of the switches and solve this problem of power dissipation. Furthermore, the hard-switching converters have other disadvantages such as limited frequency, high EMI, high switching losses, large size, and heavy weight. Two more problems are encountered during the control of the transferred power; the first one is the generated noise during the switching process while the second one is the energy lost in the switches.

Regardless of these drawbacks, this study implemented the hard-switching transitions [12]. The voltage and the active switches' current were modified to overcome or minimize their effects [13]. These modified methods work by either forcing the voltage across the switch or current through the switch to zero, and such a transition technique can only be achieved with a soft-switching technique (**Figure 2**). The current waveform is forced to reduce to 0 in the zero current switching (ZCS) circuit while the voltage waveform is treated as such by the zero voltage switching (ZVS) circuit. Power circuits with these types of transition techniques are called soft-switching converters (SSCs) [14]. Meanwhile, there are

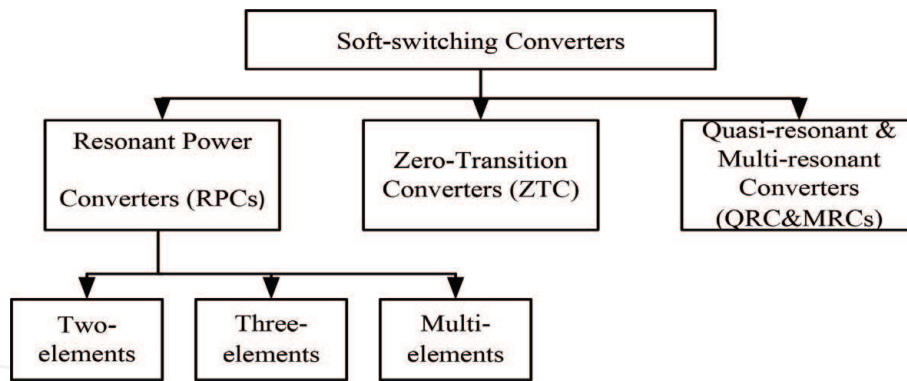


Figure 3.
 Categories of the SSCs.

several advantages of the SSCs over the linear mode regulators. The advantages include (i) the possibility of using a small ferrite transformer core due to the high-switching frequency, making operation in a wider DC input voltage range possible compared to the linear regulators; and (ii) it offers a higher efficiency. However, the complexity of the control circuit is associated with several drawbacks compared to the linear control circuit; and the power switching technique may increase the supply noise.

The SSCs have been significantly improved in the areas of switching losses, the EMIs, and device stresses, allowing the converters to perfectly work even at higher frequencies and a consequent reduction in the magnetic components. Generally, the SSC families are categorized into resonant transition converters (RTCs), resonant power converters (RPCs), quasi-resonant converters (QRCs), and multi-resonant converters (MRCs) based on their modes of operation, as shown in **Figure 3**.

2. Resonant power converters (RPCs)

Figure 4 shows the structure of the RPCs and each stage represents a specific job to be carried out. The controlled switching network (CSN) is powered by the DC source; it rapidly switches on and off depending on the working frequency to generate the output voltage or current, which feeds the next stage. The sinusoidal voltage and current signals are generated at a stage of the high-frequency resonant tank network (RTN), where there are two or more reactive components. This is to ensure a reduced electromagnetic interference and harmonic distortion [15]. Being deployed as an energy cushioning stage between the load and the CSN, a frequency-selective network can identify this stage. The impedances of both capacitance and inductance at resonance condition are equivalent and will produce the resonant

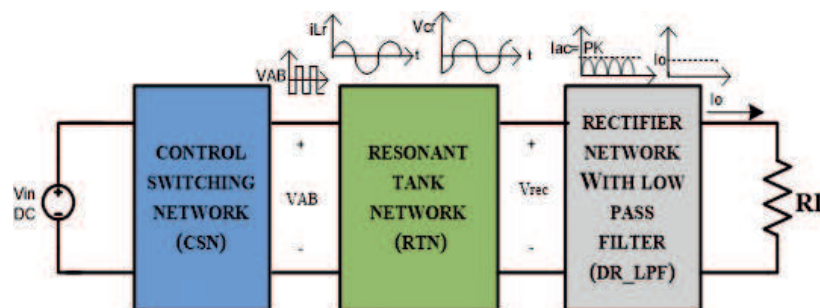


Figure 4.
 The structure of the RPC.

frequency. A rectifier network and a pass filter are then used for rectifying and filtering the output signal to generate the anticipated DC output voltage [16].

2.1 Control switching network (CSN)

The full and half bridge are the commonest switching networks, whose usage is power-dependent. For high-power applications, the full bridge inverter is often used as opposed to the single ended or half bridge inverters, which can only supply the active switch with half of the input voltage. This indicates that full bridge inverters have a low rate of voltage switch, making them ideal for application in high input voltage conditions [17]. The RPCs and either a half or full-bridge inverter are often deployed together along with each of center-tapped or full-bridge rectifiers [18].

The CSN depicted in **Figure 5** generates a square waveform voltage $V_s(t)$ of the switching frequency f_s ($\omega_s = 2\pi f_s$) as represented in Eq. 1 by the Fourier series. Considering the response of the resonant tank, which is dominant to the basic constituent f_s of the voltage waveform $V_s(t)$, then, the infinitesimal response clearly demonstrated the harmonic frequencies $n f_s$, $n = 3, 5, 7, \dots$. As a result, the power that correlates to the basic voltage waveform constituent $V_s(t)$ is moved to the resonant tank as represented in Eq. (2). The basic constituent is a sinusoidal waveform with a peak amplitude of $(4/\pi)$ times the DC source voltage. This basic constituent and the original waveform are in the same phase. However, when the S1 is on, there is a positive output sinusoidal switched current (t) but negative when S2 is off. This is due to the alternate working principle of the two switches, and its peak amplitude I_{s1} with phase equal to ϕ_s . The input current (DC) to the CSN can be computed by dividing the sinusoidal switched current with half the switching period [6, 16].

$$V_s(t) = \frac{4V_g}{\pi} \sum_{n=1,3,5,\dots} \frac{1}{n} \sin(n\omega_s t) \quad (1)$$

$$V_{s1}(t) = \frac{4V_g}{\pi} \sin(n\omega_s t) \quad (2)$$

$$i_s(t) = I_{s1} \sin(\omega_s t - \phi_s) \quad (3)$$

$$I_{in} = \frac{2}{T_s} \int_0^{\frac{T_s}{2}} i_s(t) dt = \frac{2}{\pi} I_{s1} \cos(\phi_s) \quad (4)$$

2.2 Resonant tank network (RTN)

Resonant tank networks (RTNs) comprise of LC circuit (reactive elements) that stock oscillating energy with the frequency of circuit resonant. The LC circuit's resonance h attains the electromagnetic frequency useful in several applications, including the telecommunication technology. The tank can possibly be charged to a

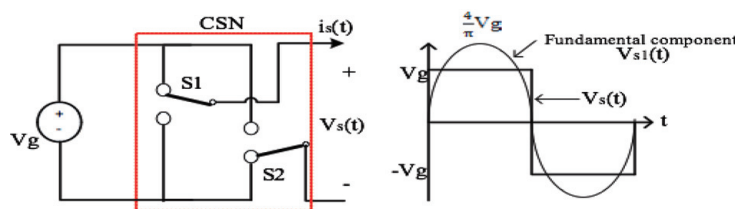


Figure 5.
The equivalent circuit of CSN.

certain resonant frequency through the adjustment of reactive element data. In addition, the essential phase of the resonant power converter is the resonant tank network. There are different kinds of RTN; it is mainly categorized into three parameters. Firstly, the resonant power converter can be sectioned through the connection technique used in tank element. The main common three resonant circuits include a series-parallel resonant converter (SPRC), a series resonant converter (SRC), and parallel resonant converter (PRC) [19]. The second factor lies in a quantity of the reactive elements (amount of transfer function order). However, the third one depends on the elements and multi-elements resonant tank [16]. Topographies of the three elements RTN (third order resonant tank) are controlled in overpowering the inadequacies in the two elements RTN. Most especially, the third element is put in the two elements RTN with a certain rumination to generate the three elements RTN. Thus, these can be taken as an integration of the advantages of mostly used two elements resonant converters PRC and SRC and enhance their inadequacies. The third order RTN contains 36 various tanks, the most common used tanks are LCC, LCL, and CLL [14, 20]. Multi-element resonant converters are RTN that contains four and beyond the number of elements. It should be noted that an increase in the number of reactive elements cause the network to be more complicated based on its size, analysis, and cost. For instance, **Figure 6** illustrates the fourth order RTN, which is referred to as the LCLC tank system [21]; this topology includes the characteristics of two main famous three-element systems such as LLC and LCC, and then reflects on their setbacks.

2.3 Diode rectifier network with low pass filter (DR-LPF)

The RTN generates voltage waveforms and sinusoidal current based on the output voltage and resonant frequency, which are taken to be the input to the last phase DR-LPF is the pulse waveform. This implies that the purpose of utilizing DR-LPF is to filter and correct the AC waveform to achieve the entailed DC output waveform. In the previous studies on resonant power converter, the DR-LPS had been illustrated as a full-bridge or center-tapped rectifiers. While the center-tapped rectifier is inappropriate due to an elevated voltage stress from the diodes, the low pass filter had been investigated for the entire occurrences of inductance or capacitive [16, 22].

2.3.1 Diode rectifier with capacitive low pass filter (DR-CLPF)

In the DR-CLPF, the input voltage $V_R(t)$ is appraised as the square wave of a resonant frequency as illustrated in **Figure 7**. The input voltage $V_R(t)$ can be estimated based on the resonant tank filtering with its basic component $V_{R1}(t)$ as shown in Eqs. (6) and (7), respectively. In addition, the basic component and current are in the same phase, any drop in current to zero alters the basic compartment because of the variations in the conducting diodes.

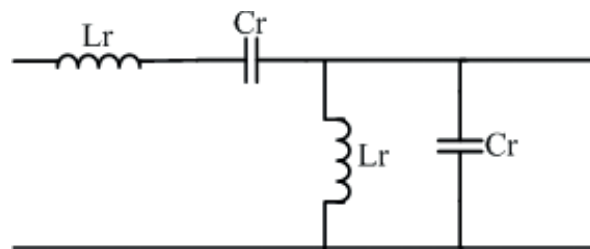


Figure 6.
An illustration of four-element RTN (LCLC).

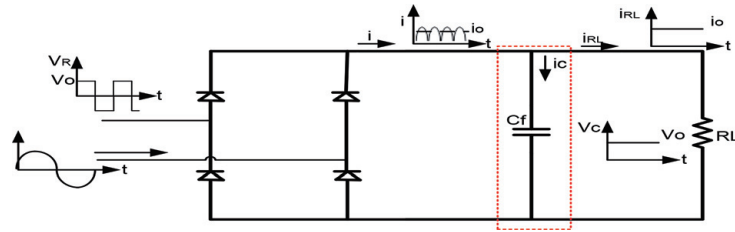


Figure 7. DR-CLPF containing a capacitive pass filter and its variables waveforms.

$$i_R(t) = I_p \sin(\omega_s t - \phi_s) \quad (5)$$

$$V_R(t) = \frac{4V_o}{\pi} \sum_{n=1,3,5,\dots} \frac{1}{n} \sin(n\omega_s t - \phi_s) \quad (6)$$

$$V_{R1}(t) = \frac{4V_o}{\pi} \sin(\omega_s t - \phi_s) \quad (7)$$

$$I_o = \frac{2}{T_s} \int_0^{T_s/2} i_R(t) dt = \frac{2}{\pi} I_R \quad (8)$$

2.3.2 Diode rectifier coupled with inductive low pass filter (DR-LLPF)

The diode rectifier is coupled with the input voltage $V_R(t)$ (sinusoidal waveform) and an inductive filter jacket. The current inputted is appraised as the square waveform $i_R(t)$ as illustrated in **Figure 8**.

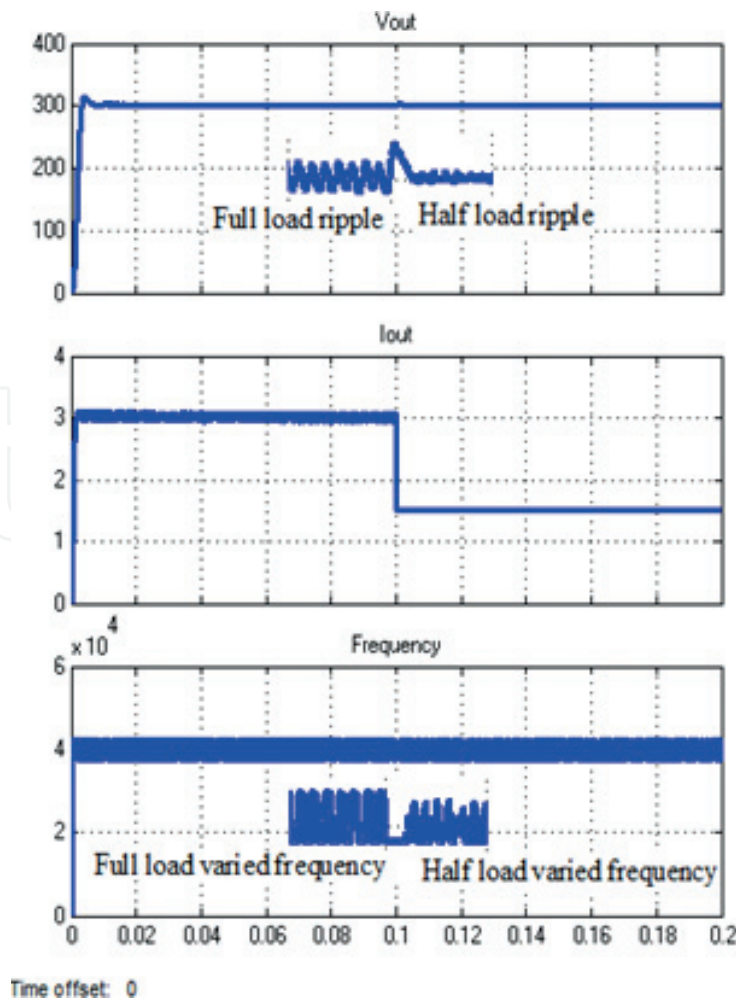


Figure 8. DR-LLPF coupled with an inductive pass filter and its variables waveforms.

$$V_R(t) = V_p \sin(\omega_s t - \varphi_s) \quad (9)$$

$$i_R(t) = \frac{4I_o}{\pi} \sum_{n=1,3,5,\dots} \frac{1}{n} \sin(n\omega_s t - \varphi_s) \quad (10)$$

$$i_{R1}(t) = \frac{4I_o}{\pi} \sin(\omega_s t - \varphi_s) \quad (11)$$

$$V_o = \frac{2}{T_s} \int_0^{\frac{T_s}{2}} V_R(t) dt = \frac{2}{\pi} V_R \quad (12)$$

3. Properties of resonant power converters

3.1 Parallel resonant converter (PRC)

The PRC is categorized into two elements tank converter. The resonant capacitor C_r needs to be parallel to the diode rectifier network DR and load. For the effective load resistance, R_{ac} is much more enormous relative to resonant capacitor reactance C_r ; this implies that the resonant current is unproportionable to the load. Moreover, in addition, the voltage over the resonant capacitor and parallel resistance R_{ac} can be improved by declining the load [14]. **Figure 9** shows the relationship between the load quality factor and PRC voltage gain depending on switching frequency based on Eq. (13). It can be observed that the high voltage gain is attained from the switching frequencies and light load conditions, which are nearly equivalent to resonant frequency $f_s = f_r$. Therefore, PRC can either step the output voltage down or up depending on the variation in the control switching system frequency. The voltage output can be adjusted with load states, whereas, the resonant current is restricted to resonant inductor data, this causes the PRC to be appropriate for open and short circuit applications [23].

$$M_V = \frac{1}{\sqrt{\left[1 - \left(\frac{f_s}{f_r}\right)^2\right]^2 + \left[\frac{f_s}{f_r} \left(\frac{1}{Q}\right)\right]^2}} \quad (13)$$

3.2 LLC resonant converter

LLC resonant converter in the RTN comprises three reactive elements, whereby it is appraised as a conventional SRC and addition of inductor L_r equidistant to the

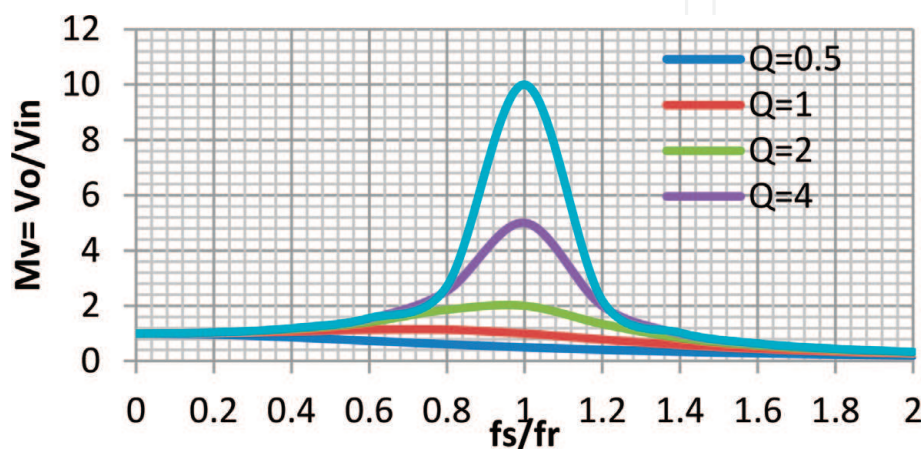


Figure 9.
Voltage gain characteristic of PRC.

load that is referred to as parallel inductor L_{rp} . The parallel inductor can be replaced by using the magnetizing inductance when using a transformer [14, 16]. The topology of LLC generates two resonant frequencies: firstly, the series resonant frequency f_{r1} depending on the series elements L_r C_r and secondly, the parallel resonant frequency f_{r2} depending on the entire three tank elements (L_{rp} , C_r , and L_r) as illustrated in Eqs. (14) and (15), where $f_{r1} > f_{r2}$.

$$f_{r1} = \frac{1}{2\pi\sqrt{(L_r + L_{rp})C_r}} \quad (14)$$

$$f_{r2} = \frac{1}{2\pi\sqrt{L_r C_r}} \quad (15)$$

Figure 10 illustrates the LLC voltage gain depending on the unity inductance ratio ($AL = 1$), switching frequency, and load quality factor as shown in the Eq. (16).

$$M_V = \frac{1}{\sqrt{\left[1 - \left(\frac{f_s}{f_r}\right)^2\right]^2 + \left[\frac{f_s}{f_r} \left(\frac{1}{Q}\right)\right]^2}} \quad (16)$$

3.3 LCC resonant converter

The topology of LCC in the RTN comprises three reactive elements, the capacitor C_{rp} that is connected to the load in parallel represents the third element. Thus, the topology contains two resonant frequencies: firstly, the series resonant frequency f_{r1} depending on the series elements L_r C_r and secondly, the parallel resonant frequency f_{r2} depending on the entire three tank elements (L_{rp} , C_r , and L_r) as illustrated in as they are shown in Eqs. (17) and (18), where $f_{r1} < f_{r2}$.

$$f_{r1} = \frac{1}{2\pi\sqrt{L_r C_r}} \quad (17)$$

$$f_{r2} = \frac{1}{2\pi\sqrt{L_r \left(\frac{C_r C_{rp}}{C_r + C_{rp}}\right)}} \quad (18)$$

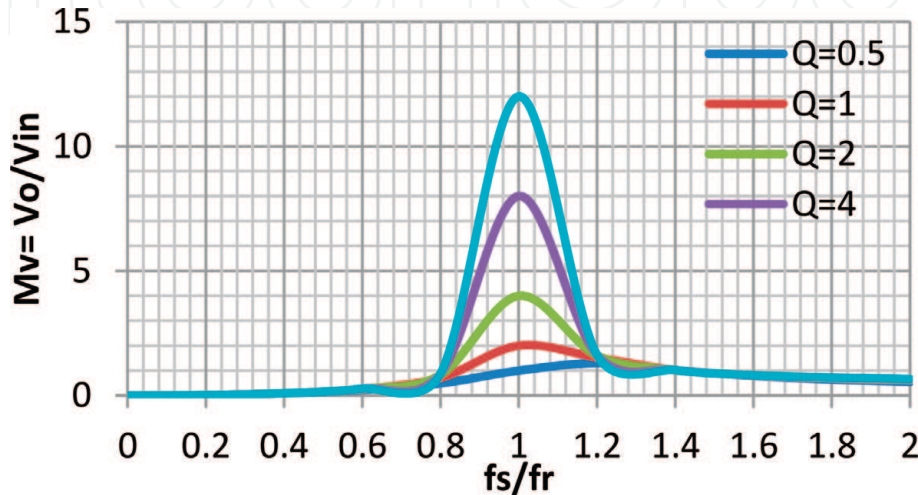


Figure 10.
Voltage gain property of LLC converter.

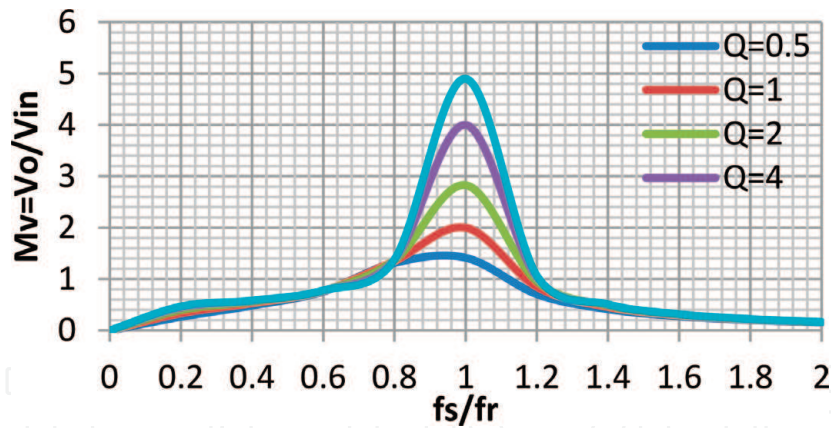


Figure 11.
 Voltage gain property of LCC converter.

In the LCC converters, the proportion of resonant capacitors A_C should be chosen prudently to be equal to the targeted peak gain. **Figure 11** explains the LCC voltage gain as depending on the load quality parameter and switching frequency with single inductance ratio ($A_C = 1$) as described in Eq. (19). It is seen that the light load voltage gain advances across the converter properties and parallel resonant frequency f_{r2} acts as a parallel resonant converter PRC.

$$M_V = \frac{1}{\sqrt{(1 + A_C)^2 \left[1 - \left(\frac{f_s}{f_{r2}}\right)^2\right]^2 + \left[\frac{1}{Q} \left(\left(\frac{f_s}{f_{r1}}\right) - \frac{A_C f_{r1}}{A_C + 1 f_s}\right)\right]^2}} \quad (19)$$

3.4 LCLC resonant converter

Similar to LCC, the topology of LCLC in the RTN comprises four reactive elements as illustrated in **Figure 6**, where this topology homogenizes the characteristics of LLC and LCC. The topology structure comprises parallel resonant capacitor C_{rp} , parallel resonant inductance L_{rp} , and a series elements $L_r C_r$, which implies that the topology contains two proportions whereby the inductance A_L and capacitance A_C must be appraised in the design. Moreover, the topology comprises three frequencies: two parallel frequencies f_{rp1} , f_{rp2} , and one series resonant frequency f_{rs} . **Figure 12** reflected the relationship between the load quality factor, $A_C = A_L = 1$ and LCLC voltage gain depending on the switching frequency as shown in Eq. (20).

$$M_V = \frac{1}{\sqrt{\left[1 + A_C + A_L - A_C \left(\frac{f_s}{f_r}\right)^2 - A_L \left(\frac{f_r}{f_s}\right)^2\right]^2 + \left[\frac{1}{Q} \left(\frac{f_r}{f_s} - \frac{f_s}{f_r}\right)\right]^2}} \quad (20)$$

4. Controlled strategies of resonant converters

The controlled strategies of the resonant converter is a bit disparate from the pulse width modulated (PWM) converters. A lot of parameters should be considered to attain a soft switching at a certain segment to fabricate the precise controller

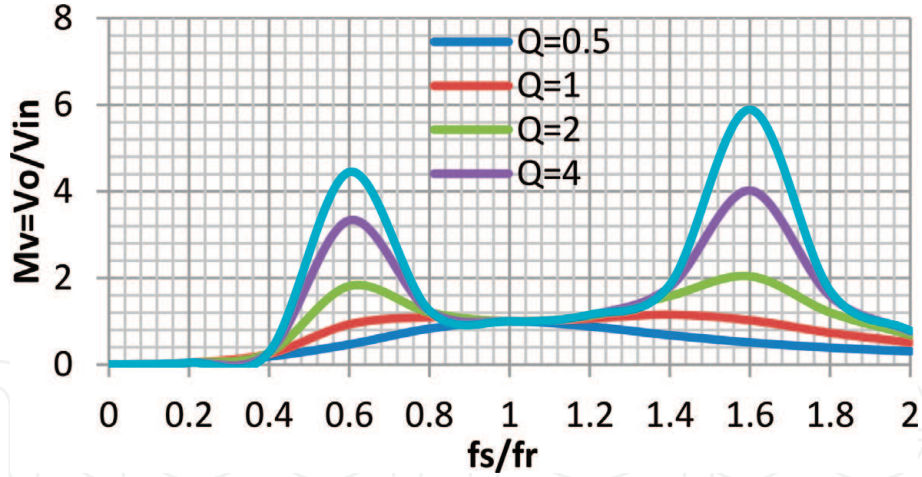


Figure 12.
Voltage gain property of LCLC converter.

that can achieve the desired results like load condition, energy storage elements, frequency range, and among others. There were several controlled topologies, which had been applied in the previous studies to manage the series resonant converters. For example, the pulse density modulation, voltage and current control, diode conduction control, and frequency control [24]. The full bridge resonant converter voltage had been regulated through the phase shift control; this phenomenon can be referred to as the switching signal primary control. In addition, to enhance the outcome of a control system, several improved techniques through adaptive controls had been reported [25], which include the passivity-based control and auto disturbance-rejection control (ADRC). A phase shift control had been used to control the current of resonant [26]. Because of this, the control outcome was increased in relative to the traditional PSRC control system. From the previous studies, the controlled techniques can be categorized into their implementation technique either through analog or digital. The digital controls are used because of their flexibility features in compact, programming, and light in comparison to analog controllers, they are also more resistant to inferences and noise. A three element DC-DC resonant converter type LLC has been discussed in this part, in order to compare the performance of frequency (duty-cycle) with variable frequency control, in terms of wide load variation.

Moreover, to ensure the expansion range of ZVS for entire inverter switches (S1–S4), and to improve the converter voltage gain. Then, the magnetizing inductance and resonant tank are used to generate a second resonant frequency

$$f_{r1} = \frac{1}{\sqrt{(L_r + L_m) \cdot C_r}}$$

From **Figure 14**, the LLC resonant converter gain M is evaluated using voltage divider law by considering the load quality factor Q and transformer step-up ratio as shown in Eq. (21).

$$M = \frac{V_o}{V_{in}} = \frac{Z_i}{Z_o} = \frac{F^2(A_L - 1)}{n \sqrt{\left(\frac{f_s^2}{f_{r2}^2} - 1\right)^2 + \left(Q(F^3 - F)^2(A_L - 1)\right)^2}} \quad (21)$$

4.1 Fixed frequency control

The purpose of using this technique is that the voltage output is being influenced by changing the duty-cycle to attain a targeted voltage output. However, the error

that exists between the constant desired voltage (reference voltage) $V_{err} = V_{ref} - V_{meas}$ and measured voltage is used for the PI controller. Thus, the controlled signal pertained to the PWM generator through the utilization of the switching frequency in generating a gate signal for the entire switches. From Eq. (21), the switching frequency that is equal to 42.5 kHz is the highest gain that can be obtained if the switching frequency and resonant frequency are closer. Therefore, a duty cycle is the only factor that measures the output voltage. Because the voltage ripple can vary by changing the load, then, the duty cycle will react to the variation of load variation relative to the estimated output voltage ripple.

4.2 Variable-frequency control

This control varies the switching frequency in adjusting the output voltage so as to reach the targeted load stage and save the output voltage of converter stable in any situation as illustrated in **Figure 5**. Moreover, the error that exists between the stable targeted voltage (reference voltage) $V_{err} = V_{ref} - V_{meas}$ and measured is used in the PI controller. Therefore, the controller increases or decreases the switching frequency based on the targeted output voltage if any variation occurs from the required output or error sign. Thus, a signal will be sent to the entire device switches. Depending on the magnetizing inductance and resonant impedance, the tank response needs to be saved inductively to appraise the attainment of the ZVS in the entire switches. However, the ranges of controlled switching frequency need to be restrained by higher and lower frequencies that affirm the fulfillment of ZVS (45 – 37.5 kHz).

4.3 Simulation results

The model simulation of resonant converter is carried out and implemented by utilizing the MATLAB/SIMULINK software using the factors enlisted in **Table 1**; this is to verify the LLC series resonant DC-DC converter design circuit as shown in **Figure 13** and control techniques analysis.

In this frequency control, the controlled signal is used for the PWM generator in generating the gate signals for the entire switches. Then, the switches S_1 and S_4 are enhanced concurrently and replace the S_2 and S_3 switches to generate the input voltage for the resonant tank V_{AB} . Therefore, the resonant elements generate the voltage V_{Cr} and sinusoidal current i_{Lr} as illustrated in **Figure 15**.

Figure 16 illustrates an output voltage of the duty-cycle controller dynamic response, the load is stepped up and down within half load of (200 Ω) and a full

V_{in}	100 (V)
L_r	200 (μ H)
C_r	70 (nF)
C_f	4.7 (μ F)
V_o	300 (V)
R_L	100 (Ω)
L_m	300 (μ H)
Kp, Ki Duty-cycle control	2.7, 0.5
f_s ranges for VF control	37.5 – 45 (kHz)

Table 1.
 The parameters of the LLC converter.

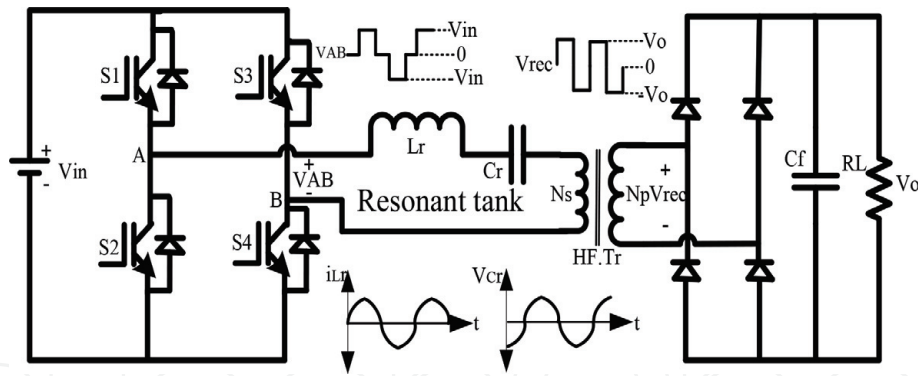


Figure 13.
A simplified illustration of full-bridge LLC resonant converter.

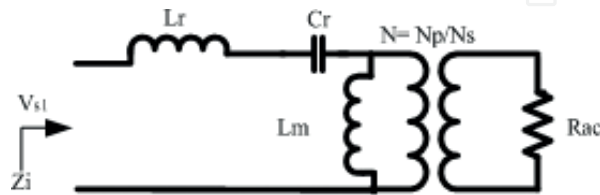


Figure 14.
The AC equivalent circuit between the rectifier and inverter.

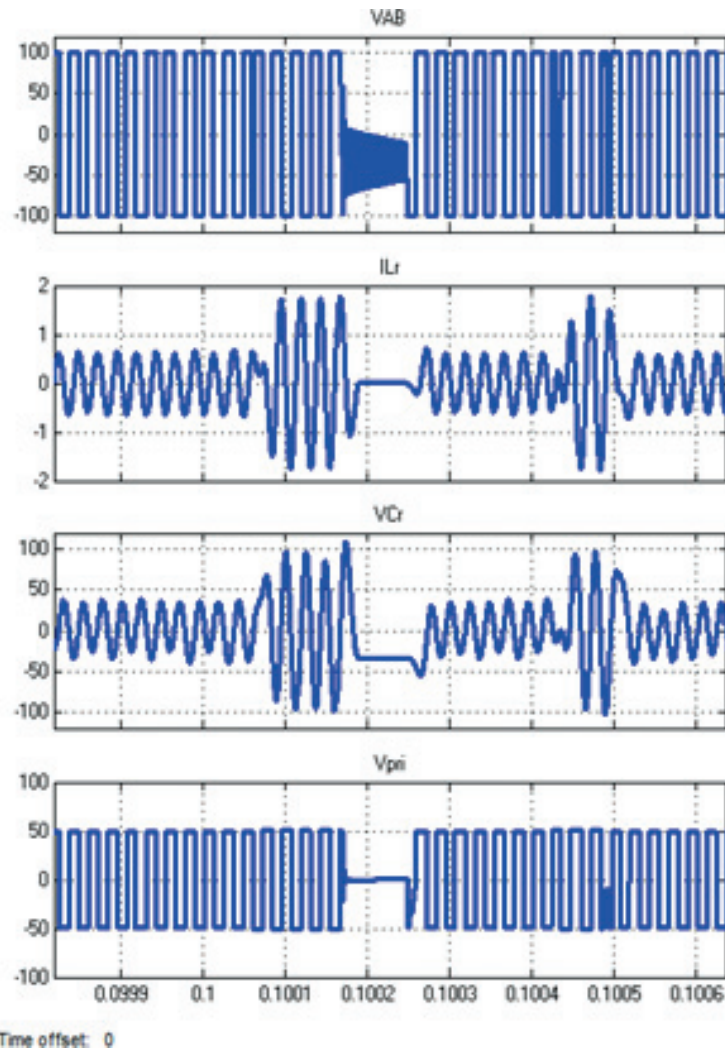


Figure 15.
Simulation waveforms of the resonant tank input voltage V_{AB} , resonant inductor current i_L , resonant capacitor voltage V_{cr} , and transformer primary voltage V_{pri} .

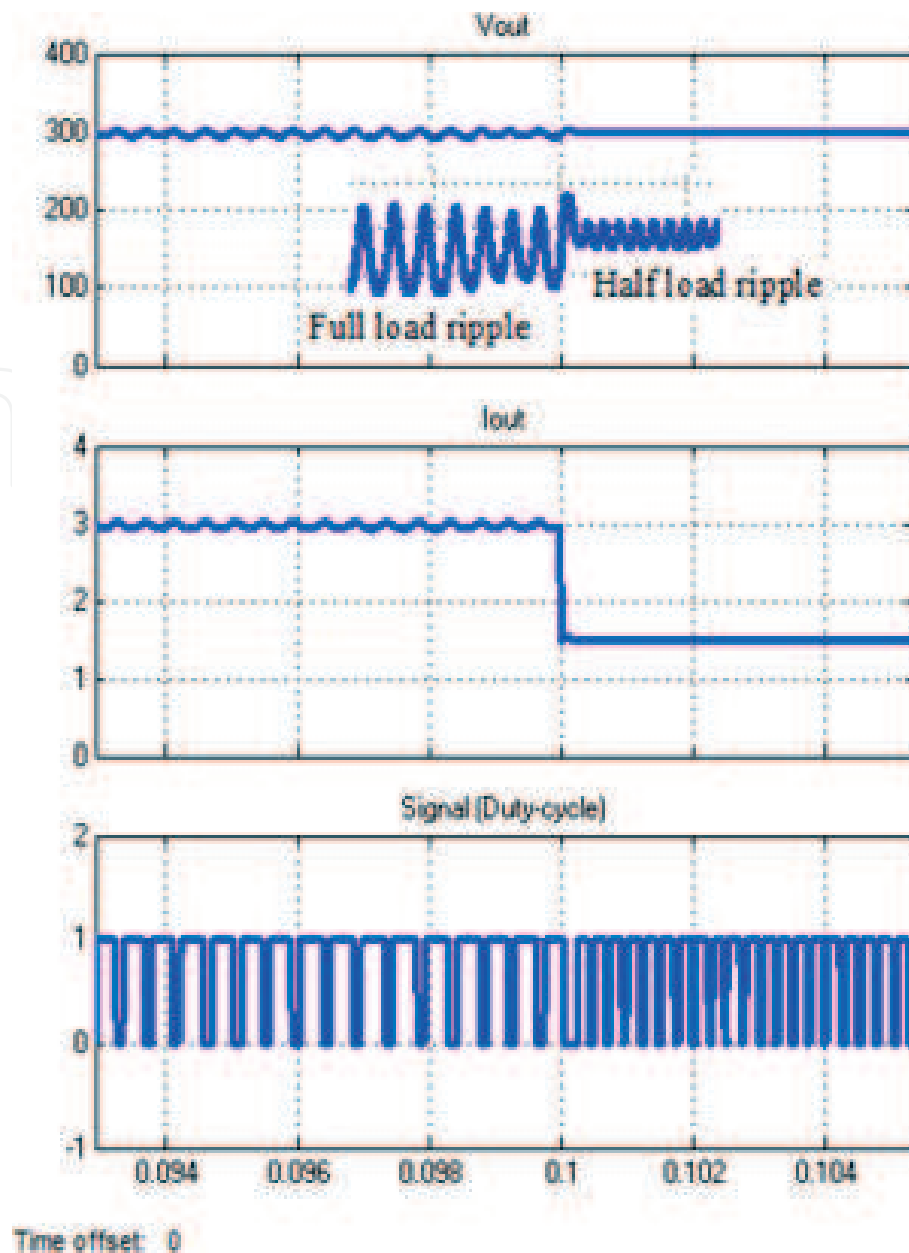


Figure 16. The dynamic response of the output voltage, output current, and controlled duty-cycle signal with respect to the load changes.

load of (100Ω). It was observed that the output voltage ripple is enormous at full load condition in relative to the half load state that reflects a direct duty cycle changes within the entire load conditions. Although, the system generates a favorable outcome by controlling the output voltage equivalent to 300 V, nevertheless, the resonant tank parameters mislaying the resonant concept during the changes in load changes as illustrated in **Figure 15**. At simulation time $t = 0.1$ s, the load varies the AC tank parameters hold-up by the $1.5e - 3$ s, thereafter, the resonant parameters reproduce the targeted AC parameters depending on a value of the load, which can be appraised as a disadvantage of the duty-cycle control technique.

In the variable frequency control technique, the measured output voltage is used to detect frequency. Thereafter, the controlled signal is implemented on PWM to produce gate signals to the entire switches by considering the switching duration depending on the converter nature to generate enormous output voltage gain. Moreover, the variation in load is being tested and applied to affirm the controller dynamic responses. **Figure 18** illustrates the parameter frequency controller dynamic response of the output voltage, and the load is stepped up and down in the

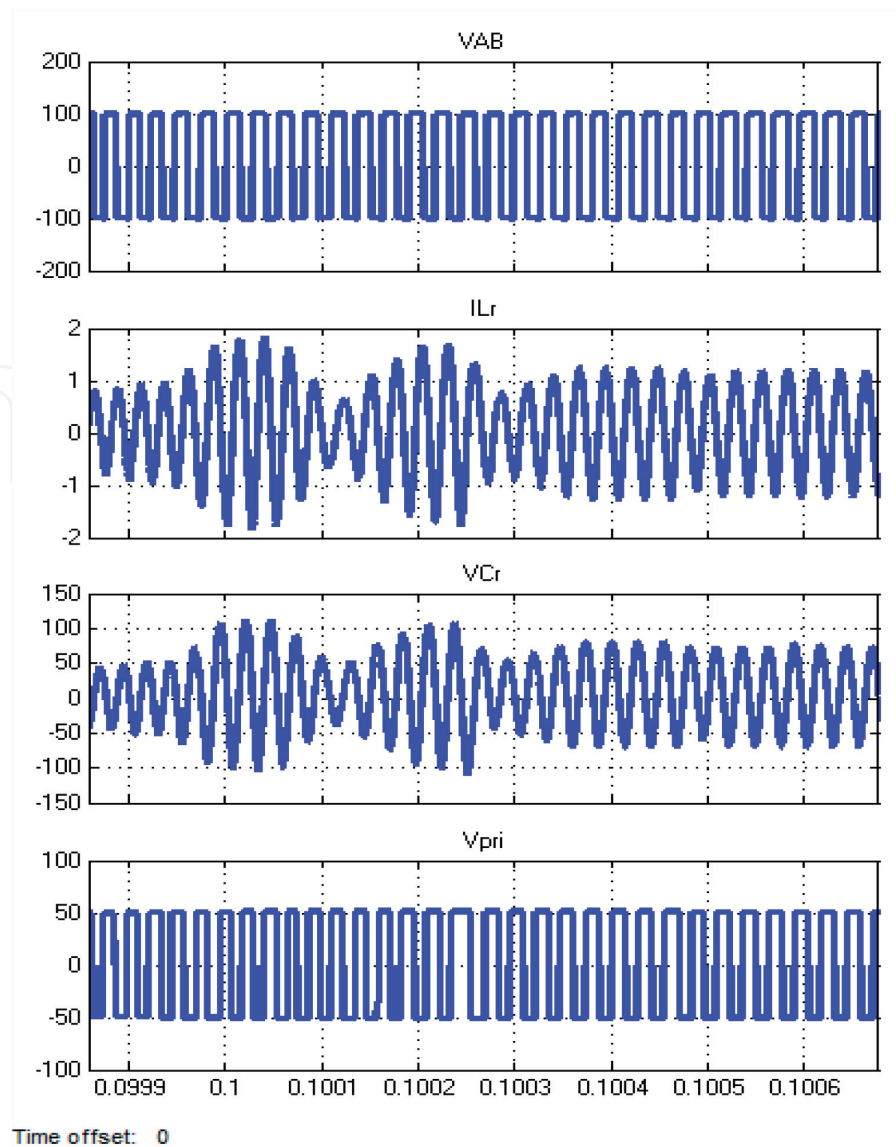


Figure 17. Simulation waveforms of the resonant tank input voltage V_{AB} , resonant inductor current i_L , resonant capacitor voltage V_{cr} , and transformer primary voltage V_{pri} .

similar way of duty-cycle control. It can also be observed that in this control technique, the full load condition results in enormous output voltage ripple as compared to half load state, and this affirms the significant variation in frequency with the entire load condition. Moreover, the parameter frequency control gives a significant response to the tank AC parameters as illustrated in **Figure 17**. As the load varies, the AC parameters temporarily react by increasing or decreasing the voltage and resonant current values depending on the varied frequency and keeping a shape of the sinusoidal waveform.

5. Applications of resonant power converters

Based on the sufficient demerit of RPCs as earlier stated in the above segments, they have uncommon application in modern industries. The summary of the noticeable implementations is discussed in this segment. The main areas of RPCs application are household applications like induction cookers, portable power supplies, network connection of renewable energy mains, and hybrid and electric vehicles. In a case of the portable power supply, requirements of the converter

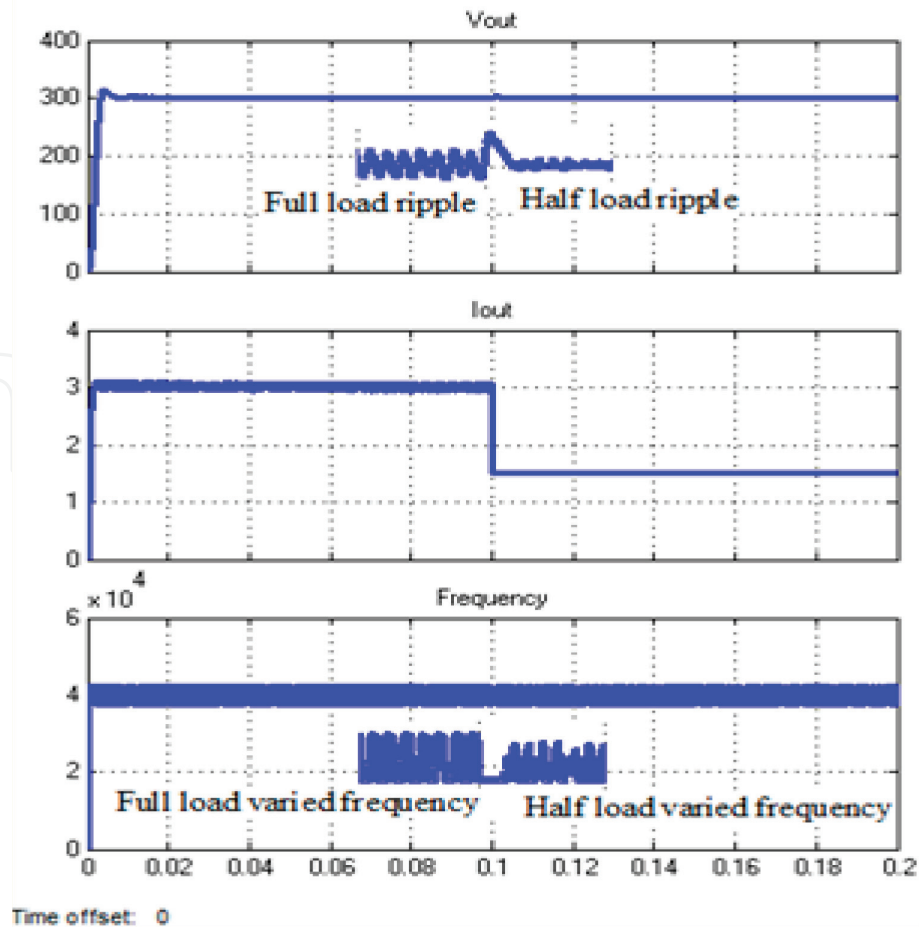


Figure 18.

The dynamic response of output voltage, output current, and controlled frequency signal as the function of load change from full to half load.

include a low price tag, light-weight and small size, high efficiency, high reliability, and low electromagnetic interference (EMI). Soft switching is the way of ensuring higher efficiency; it can be implemented by utilizing RPCs. Based on the area of application, the topology can be chosen to ensure maximum efficiency, ideal cost, and size. For example, the supply of power to an electron beam welding compartment uses a full bridge LLC resonant converter [16]. The soft switching technique and topology solves the problem associated with power utilization within the filament supply by staying away from the inverter heating challenge and ensures higher efficiencies. RPCs are used in the electrostatic precipitator. This is a high-power appliance industrially utilized for removing smoke and dust from a flowing gas. The series-parallel RPC coupled with phase control suggested by [27] is negligible in size; it gives a faster temporary response and possesses a higher efficiency as compared to the traditional line frequency power supplies. RPCs are known for charging hybrid vehicles whereby the batteries need to be charged either by wireless or wired. Due to being smaller and demonstrating higher effectiveness, the charging of EVs through wire [28] and plug-in EVs [29] RPCs are used. For example, the high-performance LLC converters are suggested in the two-stage smart battery chargers. The converter evacuates the low and frequencies ripples from the current output and increases the life of a battery without the size increment of the charger. Previous studies had proposed several wired charging topologies. Apart from wired chargers, wireless power transfer (WPT) has been a modern charging process used in the hybrid and electric vehicles. The accessible WPT technologies include electromagnetic, magnetic, and electric power transfer. Among all of these, the magnetic coupling method utilizes RPCs, which portray higher power

transmission and higher efficiency within a closer distance. Application of RPC in WPT for hybrid and electric vehicles had been reported [30].

The grid integration of renewable energy mains such as fuel cell, wind, and solar PV needs converters of minimal current ripple and higher efficiency. DC-DC converters are the main prerequisite in processing power from renewable energy mains. Out of several options, RPCs can be the main competitor because of its low EMI, higher efficiency, robustness, and low output ripple current. RPCs are used in FC networks [31, 32], PVs [33], grid connection, and electrolyser interfaces [34]. Moreover, RPCs is applied to home induction cookers. The resonant inverter is the induction cooker key element; it produces an AC current that heats up the inductor-vessel compartment. The resonant inverters utilize in induction cooker are multilevel, half bridge, single-switch, and full bridge inverters [35].

6. Conclusion

This chapter has vividly explained the resonant power converters, which include the effective generation of RPCs as a high-switching converter that can serve as a solution to electromagnetic interference (EMI) and switching losses difficulties that surface by using the PWM converters. Furthermore, the resonant converter classifications depending on several points of views as well as controlled techniques (either varied or fixed frequency techniques) were elucidated. The controlled techniques and several application areas of resonant converters have been explained. The variable and fixed frequency controls are used to cross-check the LLC converter output voltage. The load is changed when using 50% of the full load in the entire control techniques; the obtained results affirmed the significant stable response of both controllers with little overshoot voltage. Nevertheless, the variable frequency control gives a significant outcome based on the resonant tank waveforms in relative to the stable frequency control when changing the load.

Author details


Mohammed Salem^{1*} and Khalid Yahya²

¹ School of Electrical and Electronic Engineering, Universiti Sains Malaysia, Nibong Tebal, Malaysia

² Kocaeli University, İzmit, Kocaeli, Turkey

*Address all correspondence to: salemm@usm.my

IntechOpen

© 2019 The Author(s). Licensee IntechOpen. This chapter is distributed under the terms of the Creative Commons Attribution License (<http://creativecommons.org/licenses/by/3.0>), which permits unrestricted use, distribution, and reproduction in any medium, provided the original work is properly cited. 

References

- [1] Outeiro MT, Visintini R, Buja G. Considerations in designing power supplies for particle accelerators. In: Industrial Electronics Society, IECON 2013-39th Annual Conference of the IEEE 2013 Nov 10. IEEE; 2013. pp. 7076-7081. DOI: 10.1109/IECON.2013.6700307
- [2] Salem M, Jusoh A, Idris NR. Implementing buck converter for battery charger using soft switching techniques. In: Power Engineering and Optimization Conference (PEOCO), 2013 IEEE 7th International 2013 Jun 3. IEEE; 2013. pp. 188-192. DOI: 10.1109/PEOCO.2013.6564540
- [3] Mostaghimi O, Wright N, Horsfall A. Design and performance evaluation of SiC based DC-DC converters for PV applications. In: Energy Conversion Congress and Exposition (ECCE), 2012 IEEE 2012 Sep 15. IEEE; 2012. pp. 3956-3963. DOI: 10.1109/ECCE.2012.6342163
- [4] Ching TW, Chan KU. Review of soft-switching techniques for high-frequency switched-mode power converters. In: Vehicle Power and Propulsion Conference, 2008. VPPC'08. IEEE 2008 Sep 3. IEEE; 2008. pp. 1-6. DOI: 10.1109/VPPC.2008.4677473
- [5] Shafiei N, Pahlevaninezhad M, Farzanehfard H, Bakhshai A, Jain P. Analysis of a fifth-order resonant converter for high-voltage DC power supplies. *IEEE Transactions on Power Electronics*. 2013;**28**(1):85-100. DOI: 10.1109/TPEL.2012.2200301
- [6] Outeiro MT, Buja G, Carvalho A. Resonant converters for electric equipment power supply. In: Industrial Electronics Society, IECON 2014-40th Annual Conference of the IEEE 2014 Oct 29. IEEE; 2014. pp. 5065-5071. DOI: 10.1109/IECON.2014.7049270
- [7] Salem M, Jusoh A, Idris NR, Sutikno T, Buswig YM. Phase-shifted series resonant converter with zero voltage switching turn-on and variable frequency control. *International Journal of Power Electronics and Drive Systems (IJPEDS)*. 2017;**8**(3):1184-1192. DOI: 10.11591
- [8] Jin K, Ruan X. Hybrid full-bridge three-level LLC resonant converter-a novel DC-DC converter suitable for fuel cell power system. In: Power Electronics Specialists Conference, 2005. PESC'05. IEEE 36th 2005 Jun 16. IEEE; 2015. pp. 361-367. DOI: 10.1109/PESC.2005.1581649
- [9] Salem M, Jusoh A, Rumzi N, Idris N, Alhamrouni I. Steady state and generalized state space averaging analysis of the series resonant converter. In: 3rd IET International Conference on Clean Energy and Technology (CEAT). 2014. pp. 1-5. DOI: 10.1049/cp.2014.1488
- [10] Alhamroun I, Salem M, Jusoh A, Idris NR, Ismail B, Albatsh FM. Comparison of two and four switches inverter feeding series resonant converter. In: Energy Conversion (CENCON), 2017 IEEE Conference on 2017 Oct 30. IEEE; 2017. pp. 334-338. DOI: 10.1109/CENCON.2017.8262508
- [11] Rathore AK, Bhat AK, Oruganti R. A comparison of soft-switched DC-DC converters for fuel cell to utility interface application. *IEEE Transactions on Industry Applications*. 2008;**128**(4): 450-458. DOI: 10.1541/ieejias.128.450
- [12] Salem M, Jusoh A, Idris NR, Alhamrouni I. Comparison of LCL resonant converter with fixed frequency, and variable frequency controllers. In: Energy Conversion (CENCON), 2017 IEEE Conference on

- 2017 Oct 30. IEEE; 2017. pp. 84-89. DOI: 10.1109/CENCON.2017.8262463
- [13] Yang Y, Huang D, Lee FC, Li Q. Analysis and reduction of common mode EMI noise for resonant converters. In: Applied Power Electronics Conference and Exposition (APEC), 2014 Twenty-Ninth Annual IEEE 2014 Mar 16. IEEE; 2014. pp. 566-571. DOI: 10.1109/APEC.2014.6803365
- [14] Outeiro MT, Buja G, Czarkowski D. Resonant power converters: An overview with multiple elements in the resonant tank network. *IEEE Industrial Electronics Magazine*. 2016;**10**(2):21-45. DOI: 10.1109/MIE.2016.2549981
- [15] Polleri A, Anwari M. Modeling and simulation of paralleled series-loaded-resonant converter. In: Second Asia International Conference on Modelling & Simulation. 2008. p. 974. DOI: 10.1109/AMS.2008.86
- [16] Salem M, Jusoh A, Idris NR, Das HS, Alhamrouni I. Resonant power converters with respect to passive storage (LC) elements and control techniques—An overview. *Renewable and Sustainable Energy Reviews*. 2018; **91**:504-520. DOI: 10.1016/j.rser.2018.04.020
- [17] Chuang YC, Ke YL, Chuang HS, Chen HK. Implementation and analysis of an improved series-loaded resonant DC-DC converter operating above resonance for battery chargers. *IEEE Transactions on Industry Applications*. 2009;**45**(3):1052-1059. DOI: 10.1109/TIA.2009.2018946
- [18] Ivensky G, Bronshtein S, Abramovitz A. Approximate analysis of resonant LLC DC-DC converter. *IEEE Transactions on Power Electronics*. 2011;**26**(11):3274-3284. DOI: 10.1109/TPEL.2011.2142009
- [19] Salem M, Jusoh A, Idris NR, Alhamrouni I. A review of an inductive power transfer system for EV battery charger. *European Journal of Scientific Research*. 2015;**134**:41-56
- [20] Tan X, Ruan X. Equivalence relations of resonant tanks: A new perspective for selection and design of resonant converters. *IEEE Transactions on Industrial Electronics*. 2016;**63**(4): 2111-2123. DOI: 10.1109/TIE.2015.2506151
- [21] Shafiei N, Farzanehfard H. Steady state analysis of LCLC resonant converter with capacitive output filter. In: Power and Energy (PECon), 2010 IEEE International Conference on 2010 Nov 29. IEEE; 2010. pp. 807-812. DOI: 10.1109/PECON.2010.5697690
- [22] Lin BR, Hou BR. Analysis and implementation of a zero-voltage switching pulse-width modulation resonant converter. *IET Power Electronics*. 2014;**7**(1, 1):148-156. DOI: 10.1049/iet-pel.2013.0134
- [23] Salem M, Jusoh A, Idris NR, Sutikno T, Abid I. ZVS full bridge series resonant boost converter with series-connected transformer. *International Journal of Power Electronics and Drive Systems (IJPEDS)*. 2017;**8**(2):812-825. DOI: 10.11591
- [24] Salem M, Jusoh A, Idris NR, Tan CW, Alhamrouni I. Phase-shifted series resonant DC-DC converter for wide load variations using variable frequency control. In: Energy Conversion (CENCON), 2017 IEEE Conference on 2017 Oct 30. IEEE; 2017. pp. 329-333. DOI: 10.1109/CENCON.2017.8262507
- [25] Lu Y, Cheng KW, Ho SL, Pan JF. Passivity-based control of a phase-shifted resonant converter. *IEE Proceedings-Electric Power Applications*. 2005;**152**(6):2005, 1509-2015. DOI: 10.1049/ip-epa:20045261

- [26] Lu Y, Cheng KE, Ho SL. Quasi current mode control for the phase-shifted series resonant converter. *IEEE Transactions on Power Electronics*. 2008;**23**(1):353-358. DOI: 10.1109/TPEL.2007.911846
- [27] Salem M, Jusoh A, Idris NR, Alhamrouni I. Extension of zero voltage switching range for series resonant converter. In: *Energy Conversion (CENCON)*, 2015 IEEE Conference on 2015 Oct 19. IEEE; 2015. pp. 171-175. DOI: 10.1109/CENCON.2015.7409534
- [28] Musavi F, Craciun M, Gautam DS, Eberle W, Dunford WG. An LLC resonant DC-DC converter for wide output voltage range battery charging applications. *IEEE Transactions on Power Electronics*. 2013;**28**(12): 5437-5445. DOI: 10.1109/TPEL.2013.2241792
- [29] Mousavi SM, Beiranvand R, Goodarzi S, Mohamadian M. Designing A 48 V to 24 V DC-DC converter for vehicle application using a resonant switched capacitor converter topology. In: *Power Electronics, Drives Systems & Technologies Conference (PEDSTC)*, 2015 6th 2015 Feb 3. IEEE; 2015. pp. 263-268. DOI: 10.1109/PEDSTC.2015.7093285
- [30] Bojarski M, Asa E, Outeiro MT, Czarkowski D. Control and analysis of multi-level type multi-phase resonant converter for wireless EV charging. In: *Industrial Electronics Society, IECON 2015-41st Annual Conference of the IEEE 2015 Nov 9*. IEEE; 2015. pp. 5008-5013. DOI: 10.1109/IECON.2015.7392886
- [31] Outeiro MT, Carvalho A. Methodology of designing power converters for fuel cell based systems: A resonant approach. In: *New Developments in Renewable Energy*. Rijeka: In Tech; 2013. DOI: 10.5772/54674
- [32] Outeiro MT, Carvalho A. Design, implementation and experimental validation of a DC-DC resonant converter for PEM fuel cell applications. In: *Industrial Electronics Society, IECON 2013-39th Annual Conference of the IEEE 2013 Nov 10*. IEEE; 2013. pp. 619-624. DOI: 10.1109/IECON.2013.6699206
- [33] Rezaei MA, Lee KJ, Huang AQ. A high-efficiency flyback micro-inverter with a new adaptive snubber for photovoltaic applications. *IEEE Transactions on Power Electronics*. 2016;**31**(1, 1):318-327. DOI: 10.1109/TPEL.2015.2407405
- [34] Beres RN, Wang X, Blaabjerg F, Liserre M, Bak CL. Optimal design of high-order passive-damped filters for grid-connected applications. *IEEE Transactions on Power Electronics*. 2016;**31**(3):2083-2098. DOI: 10.1109/TPEL.2015.2441299
- [35] Mishima T, Nakagawa Y, Nakaoka M. A bridgeless BHB ZVS-PWM AC-AC converter for high-frequency induction heating applications. *IEEE Transactions on Industry Applications*. 2015;**51**(4): 3304-3315. DOI: 10.1109/TIA.2015.2409177